# Extended X-ray Absorption Fine Structure Analysis of Coenzyme $B_{12}$ Bound to Methylmalonyl-Coenzyme A Mutase Using Global Mapping Techniques†

**Eva Scheuring, Rugmini Padmakumar, Ruma Banerjee,* and Mark R. Chance***

*Center for Synchrotron Biosciences, Department of Physiology and Biophysics, Albert Einstein College of Medicine, 1300 Morris Park Avenue, Bronx, New York 10461, and Department of Biochemistry, University of Nebraska, Lincoln, Nebraska 68588-0664*

*Received October 8, 1996. Revised Manuscript Received September 9, 1997*[⊗]

**Abstract:** The two available crystallographic structures of cobalamin dependent enzymes, the 27 kDa fragment of the methylcobalamin-dependent enzyme, methionine synthase, from *Escherichia coli* [Drennan, C. L. et al. *Science* **1994**, *266*, 1669] and the 5′-deoxyadenosylcobalamin-dependent enzyme methylmalonyl-coenzyme A mutase from *Propionibacterium shermanii* [Mancia, F. et al. *Structure* **1996**, *4*, 339], show striking similarities despite the differences in reaction mechanism. In particular, the 5,6-dimethylbenzimidazole group is detached and replaced by a histidine group of the enzyme. Here we present an analysis of Extended X-ray Absorption Fine Structure (EXAFS) spectroscopic data for both 5′-deoxyadenosylcobalamin and aquocobalamin bound to methylmalonyl-coenzyme A mutase in the absence of substrate. The analysis is conducted with a suite of programs called AUTOFIT 1.0 [Chance, et al. *Biochemistry* **1996**, *35*, 9014], which allows an evenhanded comparison of the goodness-of-fit of the EXAFS data to a varied grid of simulations based on the *ab initio* EXAFS code FEFF 6.01. The X-ray edge data indicate an increase in effective nuclear charge of the metal ion of the enzyme bound 5′-deoxyadeonsylcobalamin compared to the corresponding free cobalamin, and the EXAFS results show small decreases in equatorial and no significant change in the Co−C bond length (despite the potential elongation of the Co−N(His) bond) upon cofactor binding to the enzyme. Thus, the change in coordination of the nitrogenous axial ligand engineered by the enzyme does not significantly contribute to a *trans* effect in the ground state. Weakening of the Co−C bond must be initiated by substrate binding. In addition, the global mapping technique resolves discrepancies between previous EXAFS results and crystallographic data on aquocobalamin.

## Introduction

Methylmalonyl-coenzyme A (M-CoA) mutase is a member of a group of enzymes that catalyzes rearrangement reactions on adjacent carbon atoms utilizing 5′-deoxyadenosylcobalamin (AdoCbl) as a cofactor (for a review on AdoCbl-dependent enzymes, see: Babior, 1988,[1] Finke, 1990,[2] and Banerje, 1997[3]). The crystal structure of the *P. shermanii* enzyme, which catalyzes the reversible isomerization of methylmalonyl-CoA to succinyl-CoA,[4,5] has been recently solved in the presence of the substrate fragment, desulfo-CoA.[6] The structure shows important similarities to the methylcobalamin-(MeCbl-)dependent enzyme methionine synthase from *E. coli*[7] despite the functional differences. In both cases the 5,6-dimethylbenzimidazole (DMB) group is detached from the Co atom, is moved into a deep pocket in the enzyme (providing much of the cofactor binding surface), and is replaced by a histidine group of the enzyme (α-subunit residue H610 in the case of M-CoA mutase). Since the binding of the cofactors are so similar, it begs the question as to what mechanistic factors govern the differential Co−C cleavage in these two systems. The crystallographic structures raise more questions than they resolve on these points. For example, examination of the MeCbl cofactor in the methionine synthase structure, at 3 Å resolution, cannot accurately reveal small, but functionally relevant changes in bond lengths with respect to the free cofactor since the rms deviations of the bond lengths are on the order of 0.2−0.3 Å. This is, of course, less precise than bond length data available from small molecule crystallography or extended X-ray absorption fine structure (EXAFS) spectroscopy. The M-CoA mutase cofactor structure shows a very long Co−N(His) bond (2.53 Å), but it was collected on a protein in which the cofactor was in a mixture of oxidation states (Co(II) and Co(III)-aquo), both inactive. Moreover, the adenosyl moiety was missing, leaving the question open as to what happens to the Co−C and Co−N(His) bonds in the active AdoCbl/M-CoA mutase complex. Is the Co−N(His) distance long as indicated by the crystallographic result or is it unaffected relative to the free cobalamin forms in the absence of the substrate? How is the Co−C bond affected? The global mapping technique is capable of addressing such questions by analyzing a large array of simulated

* Authors to whom correspondence should be addressed at the Albert Einstein College of Medicine of Yeshiva University. Phone: 718-430-4136; Fax: 718-430-8819; e-mail: mrc@aecom.yu.edu or University of Nebraska, Phone: 402-472-2941; Fax: 402-472-7842, e-mail: rbanerje@unlinfo2.unl.edu.

† Abbreviations. M-CoA, methylmalonyl-coenzyme A; EXAFS, extended X-ray absorption fine structure; XAS, X-ray absorption spectroscopy, AdoCbl, 5′-deoxyadenosylcobalamin; MeCbl, methylcobalamin; AqCbl, aquocobalamin; DMB, 5,6-dimethylbenzimidazole, ENC, effective nuclear charge.

⊗ Abstract published in *Advance ACS Abstracts*, December 1, 1997.

(1) Babior, B. M. *BioFactors* **1988**, *1*, 21−26.

(2) Finke, R. G. in *Molecular Mechanisms in Bioorganic Processes*; Royal Society of Chemistry: Cambridge, UK, 1990; pp 244−279.

(3) Banerjee, R. *Chem. Biol.* **1997**, *4*, 175−186.

(4) Eggerer, H.; Overath, P.; Lynen, F.; Stadtman, E. R. *J. Am. Chem. Soc.* **1960**, *82*, 2643−2644.

(5) Retey, J.; Lynen, F. *Biochem. Biophys. Res. Commun.* **1964**, *16*, 358−361.

(6) Mancia, F.; Keep, N. H.; Nakagawa, A.; Leadlay, P. F.; McSweeney, S.; Rasmussen, B.; Boesecke, P.; Diat, O.; Evans, P. R. *Structure* **1996**, *4*, 339−350.

(7) Drennan, C. L.; Huang, S.; Drummond, J. T.; Matthews, R. G.; Ludwig, M. L. *Science* **1994**, *266*, 1669−1674.

S0002-7863(96)03523-8 CCC: $14.00 

structures in an evenhanded fashion. The focus of this study is the structure of AdoCbl bound to M-CoA mutase compared to the free cofactor structure.

Additionally, we have successfully used the global mapping technique to explain earlier discrepancies between EXAFS and crystallographic results. Our earlier EXAFS data on free aquocobalamin (AqCbl)[8] showed a long Co−N(DMB) distance at 2.15 Å in disagreement with a recent high resolution crystal structure by Kratky et al.[9] which shows a short Co−N(DMB) distance at 1.92 Å. We have recollected the data and analyzed them using the global mapping method. Those data are also presented and compared to additional data on the AqCbl/M-CoA mutase complex.

## Materials and Methods

**Model Compounds.** AdoCbl and AqCbl·HCl were purchased from Sigma. An 8 mM AdoCbl solution sample was prepared in a mixture of 75%:25% glycerol:water. AqCbl was first recrystallized as a perchlorate salt based on the method described by Kratky et al.,[9] and an 8 mM solution sample was prepared in 75%:25% glycerol:water.

**Enzyme Sample Preparation.** The M-CoA mutase was first purified in the apoenzyme form and then reconstituted with either AdoCbl or AqCbl, and finally the free cofactor was separated from the complex by FPLC as described earlier.[10] The final concentration of the enzyme was ∼1 mM as determined spectrophotometrically. The conditions resulted in ∼1 mol AdoCbl bound per mol of heterodimer. All samples for the EXAFS studies were transferred to a sample holder, sealed with Mylar tape, and frozen in liquid nitrogen. An optical spectrum was taken before and after exposure to the X-ray beam for both enzyme and model compound samples. In each case, no changes were observed indicating that no detectable sample damage had occurred.

**Data Collection and Analysis.** The XAS data were collected at the National Synchrotron Light Source (NSLS), Brookhaven National Laboratory (Upton, NY), on beamline X-9B using a sagittally focused Si[111] crystal monochromator. Approximately 4 mrad of bending magnet radiation (horizontal divergence) was focused on a $1 \times 2$ mm$^2$ spot, the monochromated photon flux was $2 \times 10^{11}$ photons s$^{-1}$ at 100 mA beam current. A Ni mirror at an angle of 4.5 mrad was used to reject higher-order harmonic contamination. All experiments were carried out at 150 K in a closed cycle He cryostat under vacuum. EXAFS data were collected with 0.05 Å$^{-1}$ step sizes in $k$ space starting at 1 Å$^{-1}$ photoelectron energy. The signal averaging was weighted with respect to $k$, so that 2 s per point was used at $k = 1$ and 13 s per point was used at $k = 13$. Below 1 Å$^{-1}$ data were collected by counting at a specific energy for 1 s and incrementing the energy by 10 eV from 100 eV below the cobalt edge to 20 eV below the edge and then in 2.0 eV steps up to 1 Å$^{-1}$ with 2 s per point signal averaging. Edge data were collected in three regions: from 100 to 20 eV below the edge position with 10 eV steps and 1 s per point signal averaging, then from 20 eV below the edge to 20 eV above the edge with 0.5 eV steps and 3 s per point signal averaging, and finally from 20 to 150 eV above the edge with 1 eV steps and 2 s per point signal averaging. A total of three to five edge scans were recorded for all samples. Six AdoCbl and AqCbl, and 15−20 AdoCbl/M-CoA mutase and AqCbl/M-CoA mutase EXAFS scans were collected. To reduce the possibility of sample degradation, several independently prepared samples were measured for each compound. In addition, the X-ray beam was moved on the samples to a fresh spot after each scan thus further minimizing the exposure time, and optical spectra were examined after XAS data was collected and no detectable sample damage was observed. Data were generally taken in the range of 150−250 mA beam current. K-α cobalt fluorescence was detected using a 13 element energy resolving Ge detector.[11] The internal count rates were kept at or less than 30 000 per second per channel to avoid saturation effects in the detector. A calibration channel was set up to detect the spectrum of a cobalt foil simultaneously with all sample spectra. This calibration channel provided a reference for the energy calibration of the sample spectra.

The experimental data were manipulated using a PC based version of the AT&T Bell Labs EXAFS package on an IBM compatible computer with math coprocessor.[12] Sharp glitches caused by non-statistical events were removed before further data processing by fitting a polynomial in the appropriate region. Data manipulation with use of a linear pre-edge fit, cubic polynomial spline background (isolated atom) substraction, wavevector cubed weighting, Fourier transformation, filter, and back-transform have all been described previously.[13−15] Fourier filtered and unfiltered data were analyzed with the program AUTOFIT (v. 1.0) as described earlier[16] using an automated refinement procedure. AUTOFIT utilizes the *ab initio* X-ray absorption code FEFF(v. 6.01)[17,18] to calculate the theoretical amplitude and phase functions. The starting structure for the calculations is generated using the molecular modeling package Chem-X (Chem-X is developed and distributed by Chemical Design Ltd., England). The structure is then altered in AUTOFIT, and an input file is generated for the FEFF calculations. In the FEFF input file only a few parameters are adjusted, such as the amplitude reduction factor ($S_o^2$) and the number of scattering paths (NLEG). The Debye-Waller parameters can be either disabled in FEFF in order to be adjusted during the fitting procedure or can be calculated in FEFF in which case they are kept fixed during the fitting procedure. Specifically, the atoms to be used in the simulation (generally 25−30 in number) for the corrin compounds are evaluated by FEFF in an initial plane wave approximation for up to five scattering "legs", and the amplitudes of those individual paths are calculated. Any contribution that is less than 2.5% of the major contribution (pyrrole nitrogen single scattering) is excluded from the final simulation.

The use of multiple scattering paths provides one of the particular advantages of *ab initio* codes. In these simulations, due to the complex ring structures involved, multiple scattering is quite important. In all cases, up to five scattering paths are utilized for all atoms (e.g., for only single scattering, NLEG is set to a value of 2). It is well-known that for corrin or pyrrole rings, a number of atoms (particularly the central metal, pyrrole nitrogens, $C_\alpha$ and $C_\beta$) form line of sight orientations near enough to linear so that the overall multiple scattering contribution is on a par with the most significant single scattering paths. This is most dramatic when the metal atom is approximately in the mean plane of the corrin ring, as is the case for all these simulations.[15,16,19] Thus, these multiple scattering paths are critical for correctly simulating complex ring systems of this type. If individual single and multiple scattering paths are examined, it is clear that the contributions of the pyrrole ring scattering, as a whole, provide the predominant contribution to the EXAFS spectrum, and thus the scattering of the pyrrole carbons as well as the coordinated nitrogens is critical in determining the metal−pyrrole nitrogen distance.[16] In these simulations, when the pyrrole nitrogens are moved, the associated coordinated carbon atoms are moved with them, as a unit.

The simulated $k^3$ weighted $\chi(k)$ data is Fourier filtered to produce the amplitude and phase functions. An identical Fourier filter window (or raw data when the window includes all the data) is used for both the experimental data and for the theoretical standards. After Fourier

(8) Sagi, I.; Chance, M. R. *J. Am. Chem. Soc.* **1992**, *114*, 8061−8066.
(9) Kratky, C.; Farber, G.; Gruber, K.; Wilson, K.; Dauter, Z.; Nolting, H.-F.; Konrat, R.; Krautler, B. *J. Am. Chem. Soc.* **1995**, *117*, 4656−4670.
(10) Padmakumar, R.; Taoka, S.; Padmakumar, R.; Banerjee, R. *J. Am. Chem. Soc.* **1995**, *117*, 7033−7034.
(11) Cramer, S. P.; Chen, J.; George, S. J.; van Elp, J.; Moore, J.; Tensch, O.; Colaresi, J.; Yocum, M.; Mullins, O. C.; Chen, C. T. *Nucl. Instrum. Methods A* **1992**, *319*, 1−3, 295−289.
(12) Scheuring, E. M.; Sagi, I.; Chance, M. R. *Biochemistry* **1994**, *33*, 6310−6315.
(13) Chance, M. R.; Powers, L.; Kumar, C.; Chance, B. *Biochemistry* **1986**, *25*, 1259−1265.
(14) Chance, M. R.; Powers, L.; Poulos, L.; Chance, B. *Biochemistry* **1986**, *25*, 1266−1270.
(15) Chance, M. R.; Parkhurst, L.; Powers, L.; Chance, B. *J. Biol. Chem.* **1986**, *261*, 5689−5692.
(16) Chance, M. R.; Miller, L. M.; Fischetti, R. F.; Scheuring, E.; Huang, W.-X.; Sclavi, B.; Hai, Y.; Sullivan, M. *Biochemistry* **1996**, *35*, 9014−9023.
(17) Rehr, J. J.; Mustre de Leon, J.; Zabinsky, S. I.; Albers, R. C. *J. Am. Chem. Soc.* **1991**, *113*, 5135−5140.
(18) Rehr, J. J.; Albers, R. C.; Zabinsky, S. I. *Phys. Rev. Lett.* **1992**, *69*, 3397−3400.
(19) Chance, M. R. Ph.D. Thesis, University of Pennsylvania, 1986; Chapter 2.

filtering the theoretical data are fit to the experimental data in *k*-space by a one-atom type fitting procedure fixing the distance ($r$) and the coordination number ($N$) and letting the threshold energy $E_o$ and in some cases the Debye−Waller factor, $\sigma^2$, to float. The goodness of fit is given in the form of the residual sum squared

$$\sum R^2 = \sum_I \{(k^3 \chi_i)_{\text{experimetal}} - (k^3 \chi_i)_{\text{simulation}}\}^2 \quad (1)$$

The error analysis is performed based on methods described earlier.[20,21] We have recently modified the equation describing the acceptance range of a particular parameter.[16] According to that, the error limit of a parameter is reached when the corresponding sum of residual square increases to

$$\sum R^2_{\text{minimum}} [1 + (N_p/N_{df})] \quad (2)$$

where $N_p$ is the number of fitting parameters and $N_{df}$ is the number of degrees of freedom of the EXAFS data calculated by the known formula

$$N_{df} = (2 \times \Delta r \times \Delta k)/\pi \quad (3)$$

For each analysis hundreds of structures were generated by varying two distance parameters at a time and after the FEFF calculations each simulated EXAFS spectrum is compared to the experimental $k^3 \chi$ data, and all fitting results are recorded in a single file. Due to the excessive demands on computer time, the three important distances are not simulated simultaneously using a large number of distance values. For example, for ten individual distances for each of three liganded atom types, this requires $10^3$ simulations (1000); this is a reasonable limit. Thus, three atom simulations with a limited number of distances are examined to account for unusual cross correlation of parameters. Due to the significant contribution of the four pyrrole rings, and the fact that they are moved as a group, any simulation that moves these atoms more than 0.05 Å away from the canonical values of ca. 1.90 Å (for corrin rings) are entirely unreasonable from the standpoint of both sum-of residuals squared and comparison of the raw EXAFS data to the simulations. Thus, we can safely find a minimum distance for the average pyrrole nitrogen distances in trials versus one fixed and one varied axial ligand distance. Invariably, the minimum distance found for the pyrrole nitrogens is virtually identical for all combinations of axial ligands examined, due to their dominating influence on the spectra.

The final results are presented in black and white 3D contour plots in which the $\sum R^2$ values are represented as shaded gray or black spots as a function of two distance parameters shown in Figures 1a,b, 2a,b, 3a,b, and 4a,b. The darker the spot the smaller the $\sum R^2$ value. White areas represent fitting results with $\sum R^2$ values higher than the listed numbers. Additional to the $\sum R^2$ criteria, only those minima with reasonable $\Delta E_0$ and $\Delta\sigma^2$ values ($\Delta E_0 < \pm 10$ and $\Delta\sigma^2 < \pm 0.01$) are accepted as possible solutions. In practice, the $\Delta E_0$ and $\Delta\sigma^2$ values were all in the range of $\pm 6$ and $\pm 4 \times 10^{-3}$, respectively.

## Results and Discussion

We have analyzed X-ray absorption edge and EXAFS data of both AdoCbl and AqCbl in free form and bound to M-CoA mutase. The X-ray edge, defined as the major peak in the first derivative spectra, shifts due to a combination of factors such as oxidation state changes and electron donating or withdrawing influences of ligated atoms.[22] We define the term effective nuclear charge (ENC) to describe the net result of these effects.[23,24] As the ENC increases (becomes more positive), the promotion of core electrons to bound or unbound states is more difficult, and thus the edge transition is observed at a higher energy. The edge position for the AdoCbl/M-CoA mutase complex is observed at 7722.8 ± 0.2 eV (data not shown). This edge position is 0.5−1.0 eV higher than the observed transition for free AdoCbl (7722 ± 0.3 eV), indicative of a more positive ENC for the cobalt ion for the enzyme as compared to the free cobalamin form. By way of comparison, the AqCbl/M-CoA edge data shows little or no shift (0 to −0.5 eV) with respect to the edge position of free AqCbl (7723.5 eV).

We have successfully used edge data in the past to provide a better understanding of enzyme-mediated interactions with cobalamin cofactors. In the case of the corrinoid protein from *Clostridium thermoaceticum*, the enzyme-bound cofactor in all three oxidation states exhibited an ENC *lower* (by 0.5−1.0 eV) than the corresponding free cobalamin.[23,24] The corrinoid protein utilizes a heterolytic cleavage mechanism for scission of the cobalt−carbon bond and forms Co(I) and a methyl cation equivalent (this is not a discrete intermediate). We have speculated that the change in ENC in those cases are the result of electron density transferred from the protein, corrin, and/or methyl group to the cobalt center making the methyl group more electrophilic to facilitate the nucleophilic attack by a methyl group acceptor on carbon monoxide dehydrogenase.[24] For the M-CoA mutase, which operates via a homolytic cobalt−carbon bond cleavage mechanism, a very different behavior is observed. In this case, the native enzyme exhibits an increased ENC on the cobalt compared to the corresponding free AdoCbl cofactor. Although an increase in ENC occurs in the transition from base-on to base-off cobalamin species,[24] the change in ENC is not consistent with such a transition in this case (see below).

In the analysis of the EXAFS spectra for the free cofactors and the enzyme complexes, starting structures for FEFF simulations based on small molecule crystallographic data were selected as follows. For the FEFF simulations and the analysis of the EXAFS data for the free cofactors we have used the crystallographic data of Lenhert[25] (AdoCbl) and of Kratky et al.[9] (AqCbl), deleting all data beyond 5 Å from the Co atom. The simulations for the model compounds provide important controls for the global mapping analysis; they show that the EXAFS spectra provide solutions consistent with the small molecule data as well as the possibility for multiple solutions. For the FEFF simulations and the analysis of EXAFS data from the M-CoA mutase complexes we have used modified crystallographic coordinates of the free cofactors also up to 5 Å from the Co atom. We have appropriately altered the structure of the free cofactors based on the knowledge that histidine residue H610 from the α-subunit of the enzyme and not the DMB group is connected as the sixth ligand to the Co atom.[6,10] All atoms of the DMB group were cut except that of the imidazole ring which fully represents $His^{A610}$ of the mutase since no additional atoms of the enzyme, other than that of the imidazole group, are present within 5 Å from the cobalt ion. We assumed the same orientation for the histidine ligand as for the DMB ligand in the free cofactor and did not alter the corrin ring prior to the simulations. The FEFF parameters were set as follows: $S_0^2 = 0.85$ (values between 0.8−1.0 are empirically set, 0.85 works satisfactorily for all types of cobalt corrin simulation[26]), NLEG = 5; the Debye-Waller parameters were set to 4 (temperature) and 1500 (Debye temperature) for all simulations and kept fixed during the fitting procedure. The above Debye-Waller parameters, selected based on earlier studies on porphyrin models,[26] provided reasonable $\sigma^2$ values ($1-4 \times 10^{-3}$) and reflected the larger thermal disorder of the adenosyl moiety with respect to the N ligands. This is in agreement with our earlier EXAFS

(20) Lytle, F. W.; Sayers, D. E.; Stern, E. A. *Physica B* **1989**, *158*, 701.
(21) Powers, L.; Kincaid, B. M. *Biochemistry* **1989**, *28*, 4461−4468.
(22) Wirt, M. D.; Sagi, I.; Chen, E.; Frisbie, S. M.; Lee, R.; Chance, M. R. *J. Am. Chem. Soc.* **1991**, *113*, 5299−5304.
(23) Wirt, M. D.; Kumar, M.; Ragsdale, S. W.; Chance, M. R. *J. Am. Chem. Soc.* **1993**, *115*, 2146−2150.
(24) Wirt, M. D.; Kumar, M.; Wu, J.-J.; Scheuring, E. M.; Ragsdale, S. W.; Chance, M. R. *Biochemistry* **1995**, *34*, 5269−5273.
(25) Lenhert, P. G. *Proc. R. Soc.* **1968**, *A303*, 45−84.
(26) Scheuring, E. Ph.D. Thesis, Albert Einstein College of Medicine of Yeshiva University, 1995; p 186.

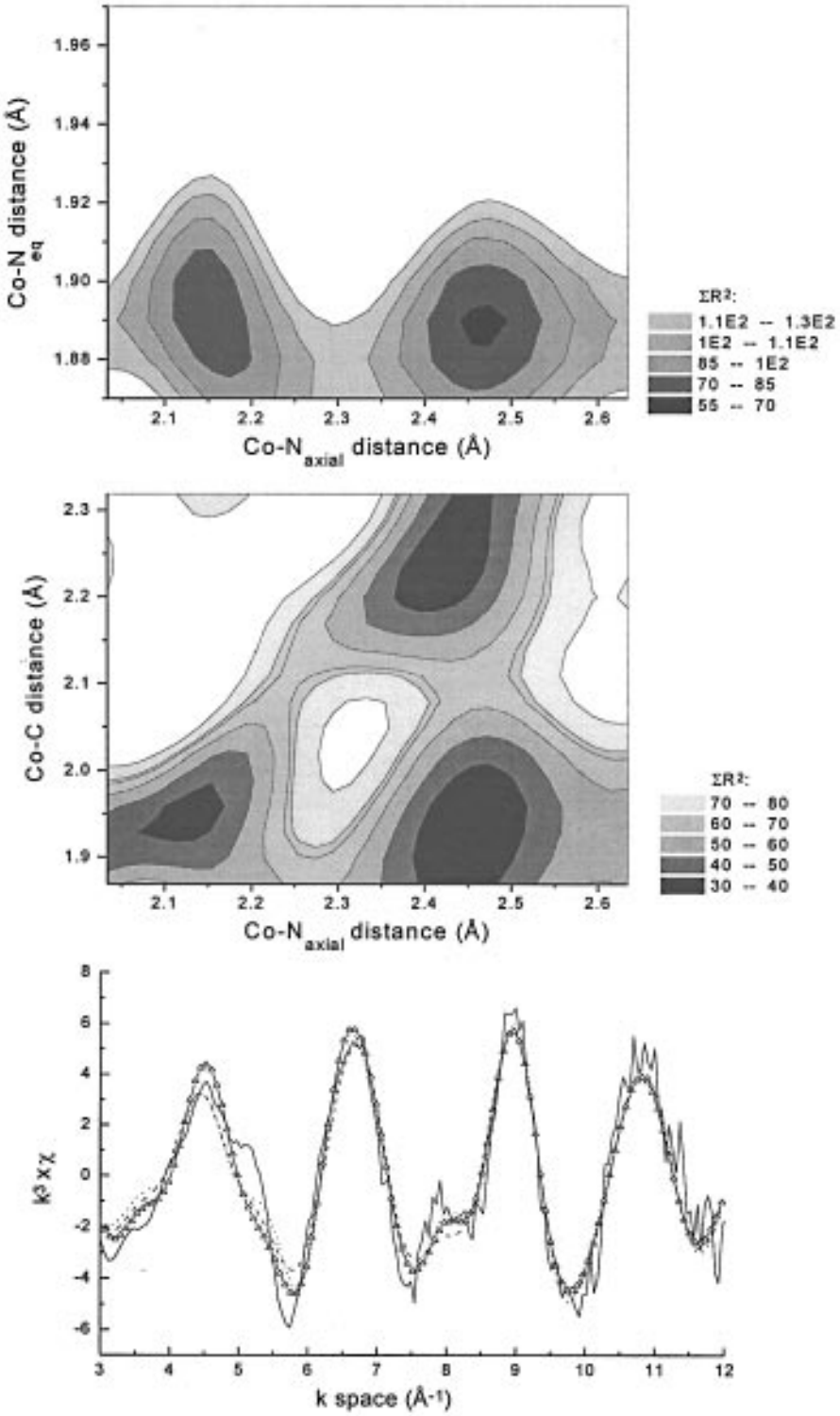


**Figure 1.** (a, top) The 3D contour plot of the AdoCbl/M-CoA simulation varying the Co−$N_{eq}$ distances from 1.87 to 1.97 Å and the Co−N(His) distance from 2.03 to 2.63 Å, leaving the Co−C bond unchanged at 2.0 Å. This simulation provides a stable minimum for the Co−$N_{eq}$ distance at 1.89 ± 0.01 Å. The simulations provide two possible minima for the Co−N(His) distance at 2.13 and 2.45 Å. (b, middle) 3D contour plot varying the Co−N(His) distance from 2.03 to 2.63 Å and the Co−C distance from 1.90 to 2.3 Å, leaving the Co−$N_{eq}$ bond unchanged at the minimum distance found at 1.89 Å. The best minimum with a Co−N(His) distance of 2.45 ± 0.05 Å and Co−C distance of 1.94 ± 0.05 Å is supported by both RR and crystallographic data. (c, bottom) The simulated EXAFS data of the three minima from part 1b compared to the unfiltered experimental $k^3\chi$data of the AdoCbl/M-CoA mutase complex (see text for details).

results on the free AdoCbl which showed higher $\sigma^2$ values for the axial C ligand than for the axial and equatorial N ligands.[27] The Fourier filter window for the models and for the experimental data were set from 0.8 to 2.8 Å for the fits represented by Figures 1b, 2b, 3b, and 4b and from 0.8 to 4.8 Å for the fits represented by Figures 1a, 2a, 3a, and 4a. Wide windows were selected for any simulation where the corrin ring equatorial nitrogens were varied, so that the single and multiple scattering contributions for all carbons of the pyrrole rings were included in the simulations. For Figures 1b, 2b, 3b, and 4b, where only the axial ligands were varied, narrowing the window emphasized the axial ligand contributions relative to the entire simulations.

(27) Sagi, I.; Wirt, M. D.; Chen, E.; Frisbie, S. M.; Chance, M. R. *J. Am. Chem. Soc.* **1990**, *112*, 8639−8644.

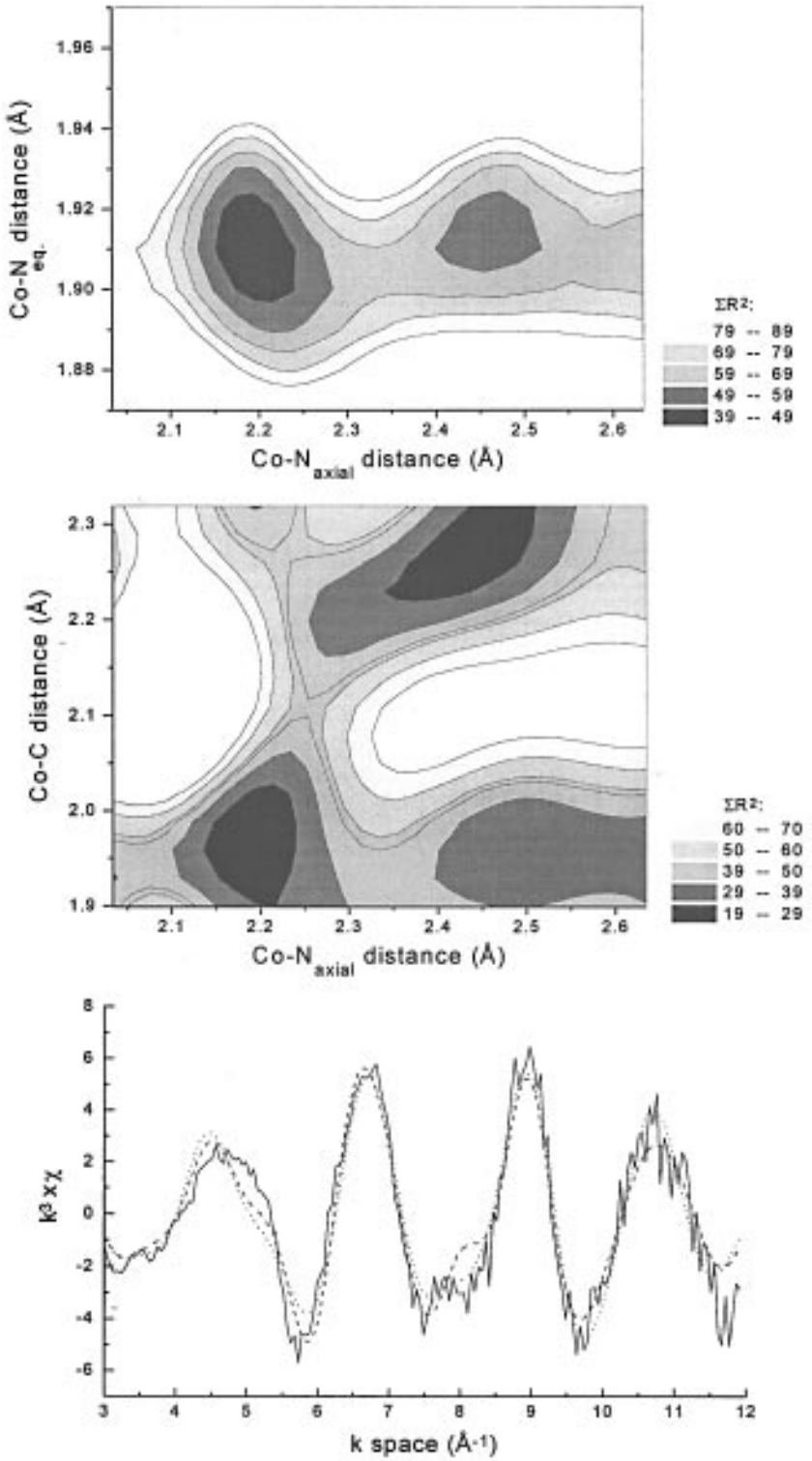


**Figure 2.** (a, top) and (b, middle) 3D contour plots of the free AdoCbl simulations. In Figure 2b the minima with the long Co−N(DMB) distances are artifacts of the EXAFS simulations and can be rejected based on the crystallographic data. (c, bottom) The simulated EXAFS data of the two minima with the best fitting results compared to the unfiltered experimental $k^3\,\chi$data of free AdoCbl (solid line: experimental data; dotted line: simulation with Co−$N_{ax}$ = 2.19 Å and Co−C = 1.99 Å; dashed line: simulation with Co−$N_{ax}$ = 2.39 Å and Co−C = 2.23 Å).

For AdoCbl we calculated that up to 3 Å the sum of the single and multiple scattering contributions from the corrin ring equals 82.5%, from the axial DMB equals 9.0%, and from the axial carbon equals 8.5% of the total EXAFS signal. Up to 5 Å, with the inclusion of single and multiple scattering from $C_\beta$ and the methine carbons, the contribution of the corrin is still 83%, while the contribution from the axial DMB group equals 10%, and the adenosyl moiety contributes 7%. Thus, the signal from the carbon axial ligand is 1.2 times greater with the narrower window. In the case of AqCbl, with the window to 3 Å, the corrin contribution equals 78.5%, the axial DMB contribution equals 10.5%, and the axial oxygen contribution equals 11%. Examining the scattering out to 5 Å, the equatorial ligand contributes 82.5%, the DMB group contributes 12%, and the axial O contributes only 5.5% to the overall EXAFS signal. In this case, the narrower window increases the contribution of the axial oxygen by a factor of 2, while the difference in the case of the carbon axial ligand is less but significant. Thus,

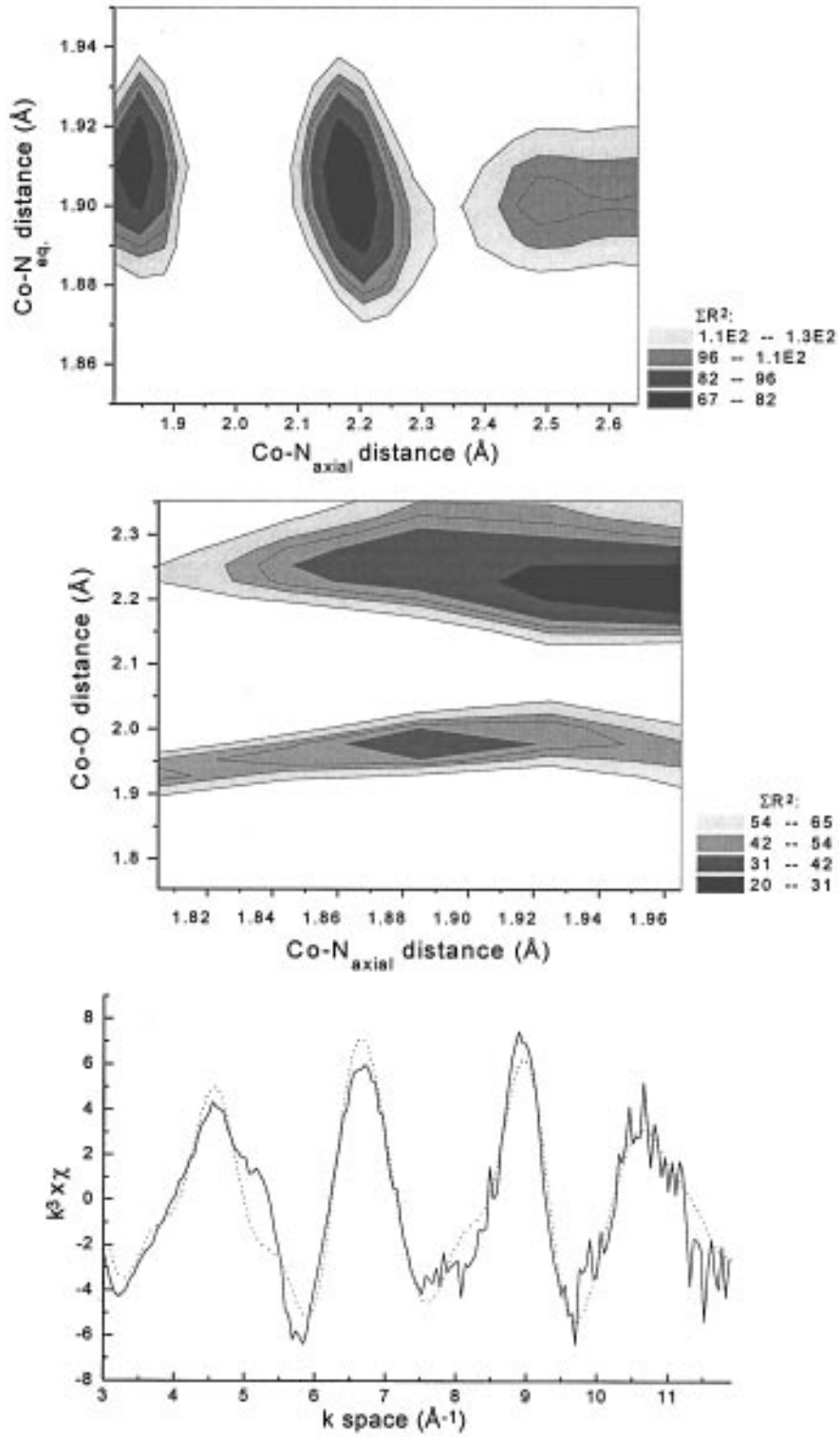


**Figure 3.** (a, top) The 3D contour plot of the AqCbl simulations varying the Co−N(DMB) distance from 2.03 to 2.63 Å and the Co−$N_{eq}$ distance from 1.85 to 1.95 Å, leaving the Co-O bond unchanged at the crystallographic minimum of 1.95 Å. This simulation provides two possible minima for the Co−N(DMB) distance from which the shorter one is supported by the crystallographic data of Kratky et al.[8] (b, middle) Simulation of the Co-O and Co−N(DMB) distances for free AqCbl provides a well resolved minimum with a Co−N(DMB) distance of 1.89 ± 0.02 Å and a Co-O distance of 1.97 ± 0.02 Å in agreement with the crystallographic solution of Kratky et al.[8] (c, bottom) The simulated EXAFS data with the minimum shown in Figure 3b compared to the unfiltered experimental $k^3\chi$data of free AqCbl (solid line: experimental data; dotted line: simulation).

we used two different Fourier-filter windows for the data analysis, a wider window (0.8−4.8 Å) to extract the Co−$N_{eq}$ distances and the smaller window (0.8−2.8 Å) to extract the Co−axial ligand distances. All data were fit in *k* space from 3.0 to 12.0 $Å^{-1}$.

To analyze the structure of the AdoCbl/M-CoA mutase complex, first the Co−$N_{eq}$ and the Co−N(His) distances were varied keeping the Co−C distance at 2.0 Å. Figure 1a represents the 3D contour plot of these simulations showing only one possible solution for the Co−$N_{eq}$ distance at 1.89 ± 0.01 Å. The Co−N(His) bond has two minima, one at about 2.15 Å and another at around 2.45 Å. Alternate simulations, where the Co−$N_{eq}$ distances and Co−C were varied, also provided the same value for Co−$N_{eq}$ (not shown). The next

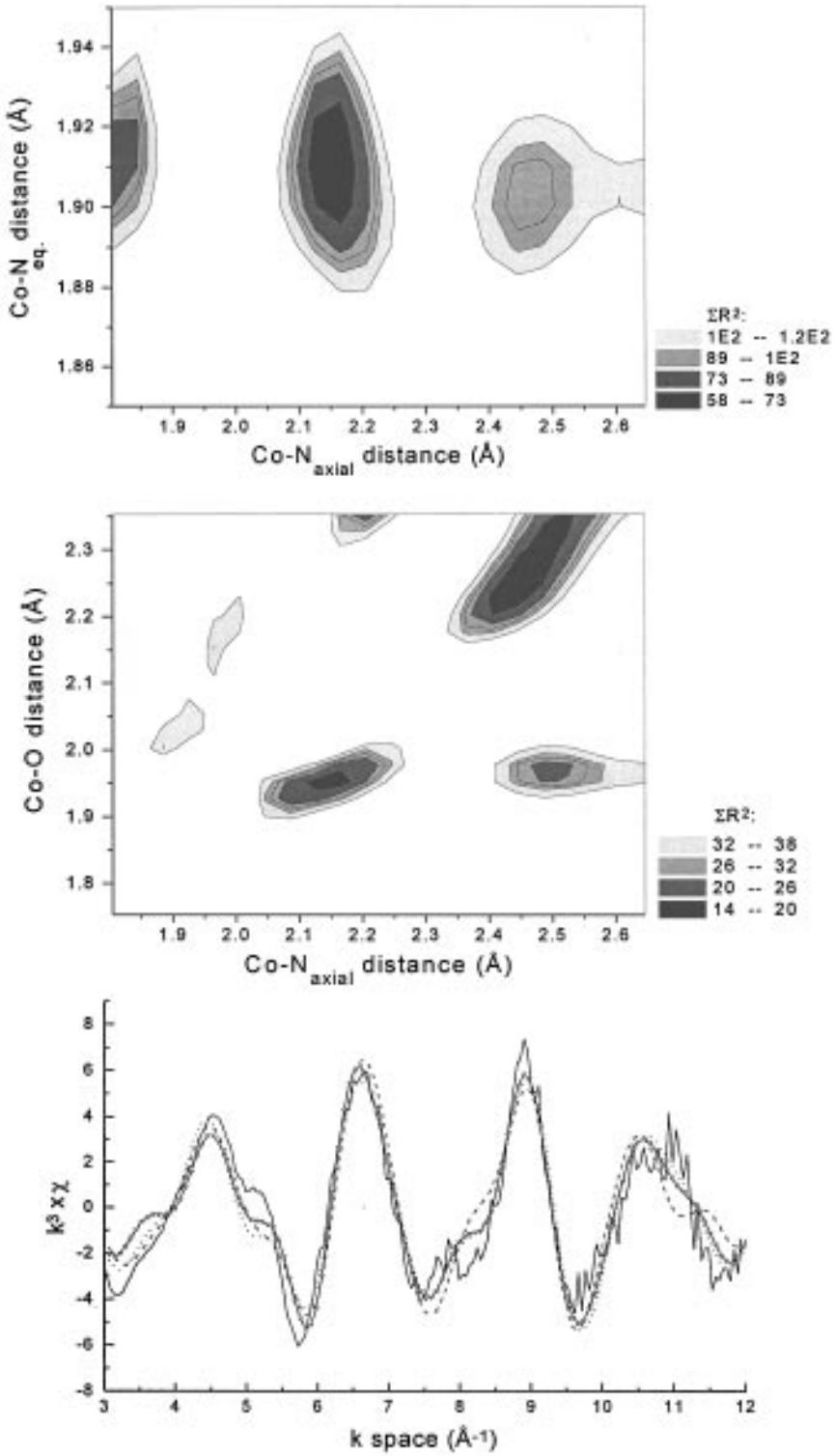


**Figure 4.** (a, top) The 3D contour plot of the AqCbl/M-CoA simulations varying the Co−N(His) distance from 2.03 to 2.63 Å and the Co−$N_{eq}$ distance from 1.85 to 1.95 Å, leaving the Co-O bond unchanged at the crystallographic minimum of 1.95 Å. This simulation provides three possible minima. (b, middle) 3D contour map produced by varying the Co−N(His) and Co-O distances keeping the Co−$N_{eq}$ distance at 1.91 Å. There are three well resolved minima with a Co−N(His) distance of 2.17 ± 0.02 Å and Co-O distance of 1.95 ± 0.02 Å ($\sum R^2$: 16), another minimum at a Co−N(His) distance of 2.49 ± 0.02 Å and Co-O distance of 1.97 ± 0.03 Å ($\sum R^2$: 16), and finally a third minimum at a Co−N(His) distance of 2.45 ± 0.05 Å and Co-O distance of 2.25 ± 0.05 Å ($\sum R^2$: 14). (c, bottom) The simulated EXAFS data with the three minima shown in Figure 4b compared to the unfiltered experimental $k^3\chi$data of the AqCbl/M-CoA complex (solid line: experimental data; dotted line: Co−N(His) = 2.17 ± 0.02 Å and Co-O = 1.95 ± 0.02 Å; dashed line: Co−N(His) = 2.49 ± 0.02 Å and Co-O = 1.97 ± 0.03 Å; and solid line with open triangles: Co−N(His) = 2.45 ± 0.05 Å and Co-O = 2.25 ± 0.05 Å).

step was to vary the Co−N(His) and the Co−C bond distances keeping the Co−$N_{eq}$ distance at the previously determined position of 1.89 Å. Figure 1b represents the solutions for these simulations. Three separate minima can be distinguished, and all are within an acceptable fitting range based on our error analysis. (Figure 1c shows the simulated EXAFS data at these three minima compared to the unfiltered experimental data (solid line)). The three minima are (i) at a Co−N(His) distance of 2.13 ± 0.04 Å and a Co−C distance of 1.97 ± 0.05 Å with a $\sum R^2$ value of 35.4 (dashed line in Figure 1c), (ii) at a Co−

N(His) distance of 2.45 ± 0.05 Å and a Co−C distance of 1.94 ± 0.05 Å with a $\sum R^2$ value of 30.4 (triangles), and (iii) at a Co−N(His) distance of 2.41 ± 0.04 Å and a Co−C distance of 2.20 ± 0.06 Å with a $\sum R^2$ value of 31.6 (dotted line). For comparison, Figure 2 shows the comparable fitting results for free AdoCbl. In Figure 2a, a minimum is seen at a Co−$N_{eq}$ distance of 1.91 ± 0.01 Å, a Co−N(DMB) distance of 2.19 ± 0.03 Å, and a Co−C distance of 1.98 ± 0.05 Å in agreement with our earlier EXAFS analysis[27] and with crystallographic data.[25,28,29] As Figure 2b shows, there are two other minima both of which can be rejected based on the crystallographic data, but one of them, the minimum with the long Co−N(DMB) and Co−C distances, cannot be rejected based on EXAFS alone (Figure 2c shows the best two simulations from Figure 2b compared to the experimental data of free AdoCbl). The presence of these additional solutions is not surprising; it is the consequence of the distance dependence of the phase of the sinusoidal EXAFS oscillation. Such multiple minima are precedented,[30] and we have recently shown their existence in the analysis of photolyzed carbonmonoxy myoglobin.[16] Based on the EXAFS data we see a small contraction of the equatorial plane, at the limit of the error analysis, for the AdoCbl cofactor upon insertion into M−CoA mutase. For the axial ligand distances the best fit ($\sum R^2 = 30.4$) provides a long Co−N(His) (2.45 ± 0.05 Å) and a slightly shorter Co−C distance (1.94 ± 0.05 Å) than in free AdoCbl (1.98 ± 0.05 Å).

Changes in ENC of the metal atom may influence the bond lengths, the canonical trans effect for cobalamins is the lengthening of the bond distance from cobalt to the DMB nitrogen in the comparison of MeCbl and AdoCbl versus AqCbl.[9,28,29,31] We have previously shown that the ENC for alkylcobalamins is lower relative to AqCbl,[22] in fact having an X-ray edge position close to cob(II) $B_{12}$ (which is shifted −1.5 eV relative to AqCbl). The lowered ENC influences the nitrogen of the DMB ligand, making it a poorer base, resulting in a weaker coordination. In the case of AdoCbl/MMCoA mutase complex, we see a small increase in ENC (relative to free AdoCbl) in the resting enzyme, which is not expected in the case of a significant lengthening of the bond to the axial base. The small decrease in the average distance from cobalt to the corrin equatorial nitrogens is consistent with the increased ENC. Yet, these comparisons to the free cobalamins presume an understanding of the bascisity of the histidine ligand provided by the enzyme. Strong hydrogen bonding to the remote nitrogen of the coordinated histidine imidazole would increase the basicity (making the nitrogen more negative) and reduce the distance from cobalt to the imidazole nitrogen as in peroxidases compared to myoglobins.[13,14] Absence of hydrogen bonding would presumably increase the Co−$N_{axial}$ distance.

In the cob(II) oxidation state, interactions between the Co and the axial nitrogen atom can be observed by EPR spectroscopy. In solution, the hyperfine coupling constant increases from ∼110 Gauss (base-on Cob(II)) to 140−160 Gauss (base-off Cob(II)) as the lower nitrogen ligand is removed by protonation.[32,33] In methylmalonyl-CoA mutase, the hyperfine coupling constant is 108 Gauss.[34] In addition, the superhyperfine coupling constants (∼19 Gauss) are comparable for the free[33] and enzyme-bound Cob(II).[34] In essence, the EPR data of the Co(II)/M-CoA species do not provide evidence for a weaker interaction. Additionally, the optical spectra for free and enzyme-bound AdoCbl have absorption maxima at 525 nm, diagnostic of a six-coordinate species with a nitrogen axial ligand. The long axial distance might be expected to induce a blue shift toward the spectrum of base-off AdoCbl which has an absorption maximum at 460 nm.[35] In summary, the EXAFS finds the most likely solution at the longer cobalt−nitrogen axial distance as suggested by the crystallographic results, but the shorter distance cannot be ruled out. The other available spectroscopic evidence provides no evidence of the weak interaction between the nitrogen and the cobalt implied by a longer distance of 2.43 Å. However, the crystal structure is of an enzyme in which substrate fragment is bound.

Using the global mapping technique we have also analyzed data of both the free and enzyme bound AqCbl. Recent high resolution crystallographic data[9] challenged our earlier EXAFS result[8] on free AqCbl with respect to axial nitrogen distance, while the Co-O and Co−$N_{eq}$ average distances were in agreement. In addition, solution NMR data was interpreted as being consistent with the crystallographic data and inconsistent with our results.[36] We have recollected the data on the perchlorate salt used by Kratky et al.[9] Our analysis, represented in Figure 3a, shows two minima for the Co−N(DMB) distance, one at a short Co−N(DMB) distance of 1.85 ± 0.03 Å with a $\sum R^2$ value of 69.0 and at a longer distance of 2.17 ± 0.04 Å with a $\sum R^2$ value of 67.2. The first solution is slightly shorter but very close to the crystallographic data (1.92 ± 0.02 Å). The second solution with the longer Co−N(DMB) distance provides the better fit with a smaller $\sum R^2$ value. This graphically illustrates why our previous results, based solely on a first shell Fourier-filter analysis, emphasized the longer distance. Variation of the Co-O and Co−N(DMB) distances for free AqCbl (shown in Figure 3b) provides a well resolved minimum with a Co−N(DMB) distance of 1.89 ± 0.02 Å and a Co-O distance of 1.97 ± 0.02 Å in agreement with the crystallographic solution of Kratky et al.[9] with a $\sum R^2$ value of 32. This simulation is shown compared to the experimental data in Figure 3c. An additional minimum can be seen in Figure 3b with long a Co-O bond which can be rejected by the crystallographic result. The improved global mapping technique reveals that multiple solutions are possible based solely on the EXAFS data. This analytical method also has the advantage of a significant excess of free parameters versus fitted parameters, while the Fourier filtered first shell data analysis had only a small excess of free parameters versus fitted parameters. This result provides confidence that the EXAFS solutions can be utilized effectively; however, they do indicate that distinctions between mathematically equivalent minima must sometimes be made and that additional information are necessary in making those choices.

Figure 4a,b represents an analysis of the AqCbl/M-CoA mutase complex varying the Co−$N_{eq}$, Co−N(His), and Co-O. The analysis provides only one minimum for the Co−$N_{eq}$ distance at 1.91 ± 0.01 Å. Variation of the Co−N(His) and Co-O distances with a Co−$N_{eq}$ distance of 1.91 Å results in three well resolved minima with a Co−N(His) distance of 2.17 ± 0.02 Å and Co-O distance of 1.95 ± 0.02 Å ($\sum R^2$: 16), another minimum at a Co−N(His) distance of 2.49 ± 0.02 Å

(28) Savage, H. F. J.; Lindley, P. F.; Finney, J. L.; Timmins, P. A. *Acta Crystallogr.* **1987**, *B43*, 280−295.
(29) Bouqiere, J. P.; Finney, J. L.; Lehman, M. S.; Lindley, P. F.; Savage, H. F. J. *Acta Crystallogr.* **1993**, *B49*, 79−89.
(30) Lee, P.; Citrin, P.; Eisenberger, P.; Kincaid, B. *Rev. Mod. Phys.* **1981**, *53*, 769−806.
(31) Rossi, M.; Glusker, J. P.; Randaccio, L.; Summers, M. F.; Toscano, P. J.; Marzilli, L. G. *J. Am. Chem. Soc.* **1985**, *107*, 1729−1738.
(32) Bayston, J. H.; King, N. K.; Looney, F. D.; Winfield, M. E. *Biochemistry* **1970**, *9*, 2162−2172.
(33) Pilbrow In *B12*; Dolphin, D., Wiley and Sons: New York, 1982; pp 431−462.
(34) Padmakumar, R.; Taoka, S.; Padmakumar, R.; Banerjee, R. *J. Am. Chem. Soc.* **1995**, *117*, 7033−7034.
(35) ) Gianotti, C. In *B12*; Dolphin, D., Wiley and Sons: New York, 1982; pp 393−430.
(36) Calafat, A. M.; Marzilli, L. G. *J. Am. Chem. Soc.* **1993**, *115*, 9182−9190.

and Co-O distance of 1.97 ± 0.03 Å ($\sum R^2$: 16), and finally a third minimum at a Co−N(His) distance of 2.45 ± 0.05 Å and Co-O distance of 2.25 ± 0.05 Å ($\sum R^2$: 14), as seen in Figure 4b. The simulated versus experimental data for these simulations are seen in Figure 4c. Note the difference from the solution patterns seen in Figure 3a,b, where the minimum with the very long Co-(DMB) distance can be clearly rejected based on the EXAFS analysis. For this analysis the short distance consistent with small molecule crystallography is excluded, while only the intermediate and longer Co−N(His) distances are consistent with the data. This and the mutase crystal structure,[6] in which a mixture of AqCbl and Co(II) are bound, also indicate the presence of a long Co−N(His) bond at 2.53 Å.

## Conclusion

The global mapping method has demonstrated that it can provide a thorough analysis of EXAFS data by comparing a large number of simulations to the experimental data in a uniform way. It allows the visualization of multiple minima in EXAFS and is able to explain discrepancies between crystallography[9] and EXAFS[8] where our earlier EXAFS analysis methods failed to provide a satisfactory solution.

In summary, our EXAFS analysis of the M-CoA mutase complexes shows only slight variation in the Co−$N_{eq}$ distances with respect to the free cofactor forms, with the possible exception of the cobalt−axial nitrogen distance, where the EXAFS data alone cannot distinguish between the two alternatives. However, the AdoCbl/M-CoA mutase complex provides a Co−$N_{eq}$ distance of 1.89 Å, slightly shorter compared to that of the free AdoCbl (1.91 Å). This is accompanied by an increase in ENC on the metal atom in the enzyme case. The AqCbl/M-CoA data shows no change in the Co−$N_{eq}$ distance with respect to free AqCbl and no changes in ENC. However, the AqCbl/M-CoA data are quite different from the free cobalamin data in that the short Co−N(His or DMB) distance found for the free cobalamin is excluded for the enzyme form.

It is noteworthy that the edge data for the mutase bound AdoCbl show a reversal in trend compared to our previous results on the corrinoid protein, where a $Co^{1+}/Co^{3+}$ cycle is initiated by heterolytic cleavage of the cobalt−carbon bond. In the latter case, all the enzyme forms examined had decreased ENC compared to the corresponding free cobalamins. In the case of the methyl-$Co^{3+}$ form, it was suggested that the lowered ENC makes the methyl group more electrophilic facilitating nucleophilic attack by the methyl group acceptor; for the $Co^{1+}$ form, the lowered ENC may make the cobalt ion more nucleophilic easing methylation and regeneration of active enzyme. For AdoCbl/MMCoA mutase, where a $Co^{2+}/Co^{3+}$ cycle is initiated by homolytic cleavage of the cobalt−carbon bond an entirely different structural and electronic mechanism is operative. The ENC is increased, and the corrin ring average distance decreases.

The EXAFS data shows multiple minima for the axial ligand distances, but we can guide our judgment using additional available information. Based on the crystallographic data of the mutase complex,[6] a longer Co−N(His) distance is expected for both the AdoCbl and AqCbl mutase complexes. For the AqCbl/M-CoA mutase complex, we see a possible solution with a Co−N(His) distance of 2.49 ± 0.02 Å and the short Co−N(DMB) distance seen in the free AqCbl form is excluded. For the AdoCbl/M-CoA mutase complex the small shift in the X-ray edge is consistent with the small shortening observed in the equatorial distances, while the optical data are not consistent with dramatic structural changes. This supports the exclusion of the EXAFS minimum with the long Co−C distance in Figure 1 which requires a dramatic change in both axial ligands, defining a Co−C distance of 1.94 Å, which is also the best EXAFS solution with the smallest $\sum R^2$ value. We can conclude that in the absence of the substrate (or a substrate analog) the Co−C bond stays unaffected and that substrate binding to the enzyme plays an important role in labilizing the cofactor toward Co−C cleavage.[37] EPR[38] and stopped-flow spectroscopic studies[39] indicate this to be the case for methylmalonyl-CoA mutase.

**Acknowledgment.** This work is supported by NIH Grants DK 45776 (R.B.), RR-01633 (M.R.C.), and HL-45892 (M.R.C.) and the Hirschl-Weil-Caulier trust (M.R.C.). M.R.C. is the holder of the Joseph and Anne Wunsch Fellowship in Biophysical Engineering from the Albert Einstein College of Medicine. The construction and operation of beamline X9B is supported by the Biotechnology Research Resource program of the National Institute of Health, P41-RR01633. The NSLS is supported by the Department of Energy, Division of Materials Sciences, Office of Energy Research.

JA9635239

(37) Weakening of the cobalt carbon bond in AdoCbl bound to the mutase has been suggested by the reported racemization at the C5′ carbon in the absence of substrate.[40] In light of this and a recent study[41] that contradicts this result, these experiments need to be repeated with highly pure recombinant enzyme.

(38) Zhao, Y.; Such, P.; Retey, J. *Angew. Chem., Int. Ed. Engl.* **1992**, *31*, 215−216.

(39) Padmakumar, R.; Padmakumar, R.; Banerjee, R. *Biochemistry* **1997**, *36*, 3713−3718.

(40) Gaudemer, A.; Zybler, J.; Zybler, N.; Baran-Marszac, M.; Hull, W. E.; Fountoulakis, M.; König, A.; Wölfle, K.; Retey, J. *Eur. J. Biochem.* **1981**, *119*, 279−285.

(41) Meier, T. W.; Thomä, N. H.; Leadlay, P. F. *Biochemistry* **1996**, *35*, 11791−11796.